Plant substances as battery cathodes: Zinc–embelin organic secondary battery

D. KALAISELVI and R. RENUKA*

Central Electrochemical Research Institute, Madras Unit, CSIR Madras Complex, Chennai 600 113, India
(*author for correspondence, fax: +91 44 2350973)

Abstract

Embelin, 2,5-dihydroxy-3-undecyl-1,4-benzoquinone a plant substance extracted from the plant *Embelier libes*, distributed in the Kerala State of India, is useful as a battery cathode material. In the present study embelin is used as a cathode in a zinc based secondary battery using $ZnCl_2$–NH_4Cl electrolyte. The battery performance is discussed in the light of cycle life of the cell under conditions of varied electrolyte composition, operational temperature and zeolite modification.

1. Introduction

Plant substances have found application in biocatalysis and sensor development [1–4]. The attractive features of plant substances are their easy preparation and low cost. Embelin, a plant substance extracted from the plant *Embelier libes*, found in the Kerala State of India, is a quinone functionality. As quinones are potential electron receptors and have known battery applications [5, 6], we examined the performance of embelin as a cathode material in a zinc based rechargeable battery system.

2. Experimental details

Embelin was an Arrow Chemicals product and was used after recrystallization. All other chemicals were E. Merck GR grade products. Double distilled water was used in preparing the solutions. The zeolite used was a calcined rare earth Y zeolite obtained by the cation exchange of commercial Y zeolite using mixed rare earth cations. The negatives were cut from 0.1 cm thick zinc sheet of 99.9% purity. Zeolite modification of embelin was made by continuously stirring a blend of 10 : 1 zeolite: embelin in benzene for 10 h. The solid was then filtered, washed and dried.

The positive plate was made by mounting a uniform mixture of PTFE binder (0.2 ml), zeolite modified (11.3 g) or unmodified (1.3 g) embelin and colloidal graphite (80 wt %) on a nickel plated mild steel mesh of dimensions $0.04 \, m \times 0.025 \, m \times 0.002 \, m$. The material was then compacted using a hydraulic press.

In the cell (Figure 1), a cathode was positioned between two zinc anodes. Direct contact of the cathode with the anodes was prevented by pasting a pair of thin PVC wires on to the inner side of the zinc sheets.

The electrolyte was composed of $ZnCl_2$ (23%) and NH_4Cl (23%) in 100 ml water. Unless otherwise specified, the battery discharge was made at a constant current drain of 50 mA. Charging was done at $C/2$ rate using a constant power supply unit (Aplab India). Separation of the electrode reaction product from the zeolite matrix was done using DMF (E Merck, GR).

Cyclic voltammograms were recorded using a PAR instrument having a potentiostat/galvanostat model 163, a current-to-voltage converter model 176, a universal programmer model 175 and a model RE 008 X-Y recorder. A platinum foil of large area was used as the auxiliary electrode (SCE) while saturated calomel electrode was used as the reference. The solutions were deaerated by passing oxygen free nitrogen through them. The cyclic voltammogram of the DMF (dimethyl formamide) extract of the cathode mix were registered using HMDE prepared by following the reported procedure of Bellamy [7]. In this study, the discharge (1st discharge) was arrested at various times, the cell was dismantled. The cathode mix was carefully separated
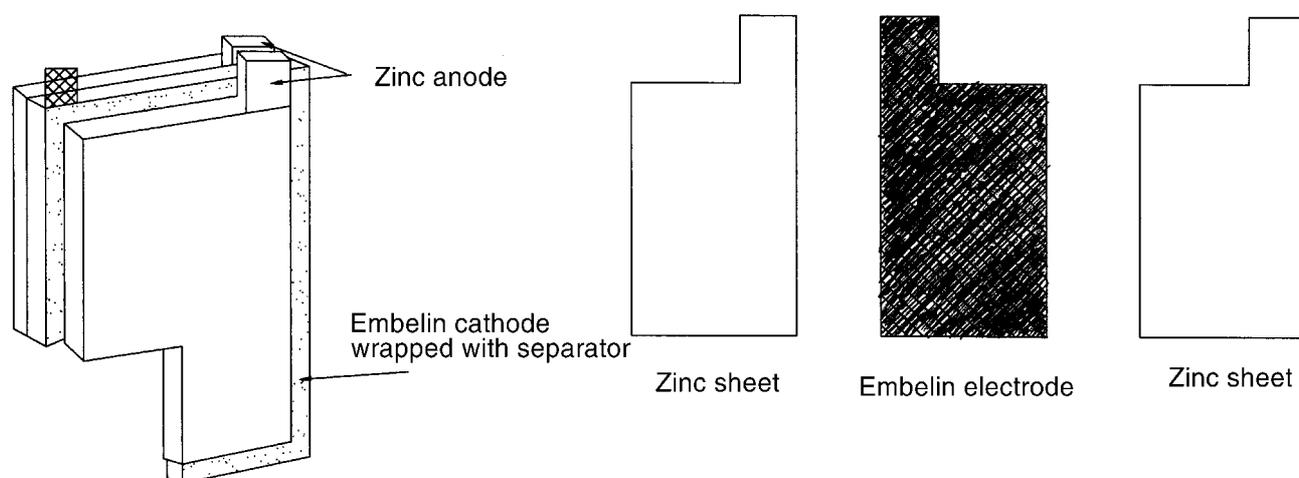
Zinc anode

Embelin cathode
wrapped with separator

Zinc sheet   Embelin electrode   Zinc sheet

Fig. 1. Zinc–embelin cell construction.

from the current collector and extracted with 25 ml of DMF. This mother extract was further diluted in an order proportionate to the time of discharge, so that that the final concentration of the material taken for analysis is atleast approximately equal in all cases and is in the 10^{-4} M range. For 30 min discharge, the mother extract was not further diluted. Whereas it was diluted 1.7 times, 2.7 times and 3.5 times, respectively, for 50, 80 and 105 min. discharges. In all cases, 5 ml of the final DMF extract was added to 50 ml of the electrolyte, namely 50% dioxane, B.R. buffer of pH 4.7.

The cyclic voltammograms were also registered for the cathode mix as such, at different stages during charging

(after washing, drying and gentle grinding in a mortar). A small quantity of cathode mix was mounted on 1×10^{-4} m^2 area gold foil using a drop of PTFE binder and compaction at 8 t pressure.

3. Results and discussion

The discharge curves for the zinc–embelin battery in 1.5 M H_2SO_4 and in $ZnCl_2$–NH_4Cl electrolyte are, respectively, shown in curves (a) and (b) in Figure 2. The pattern is typical of a quinone functionality [5, 6] in that a single step is observed in H_2SO_4 medium whereas a
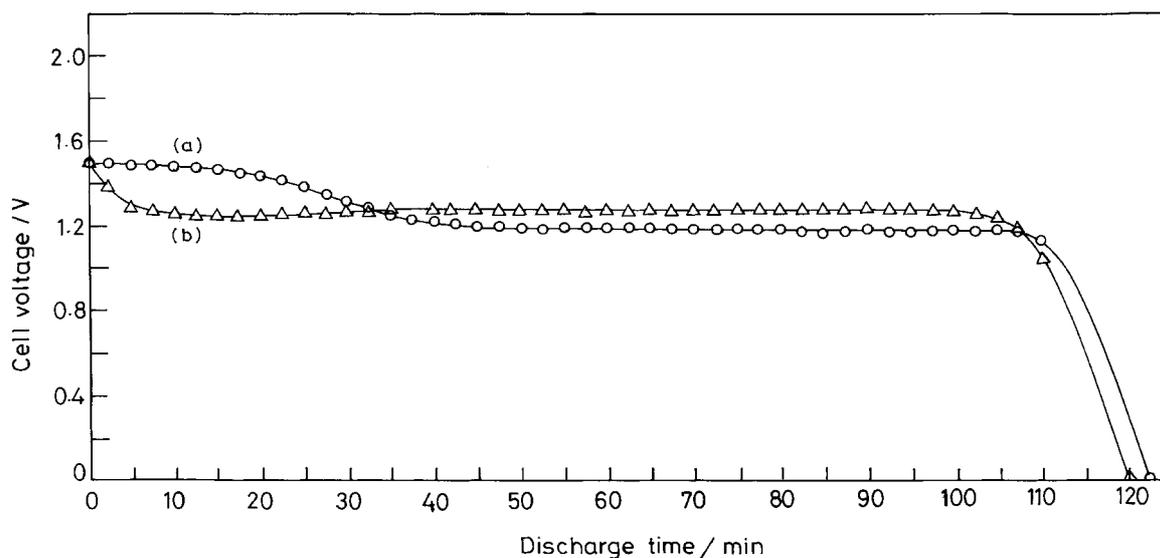

Fig. 2. Discharge curves of zinc–embelin battery. Electrolyte: (a) 1.5 M H_2SO_4 (b) $ZnCl_2$–NH_4Cl (pH 4.7). Current drain 50 mA; compaction pressure 12 t.

two step curve is observed in the ZnCl$_2$–NH$_4$Cl medium. The fundamental reaction of reduction of embelin is the 2e reduction of the quinone. In 1.5 M H$_2$SO$_4$, the reduction is seen as an overall single 2e step. At pH 4.7, a two step curve is observable owing to the stabilization of the semiquinone intermediate.

Figure 3 presents a comparison of the zinc–embelin cell with that of conventional cells of manganese dioxide coupled with magnesium or zinc. As can be seen, although the cell voltage of the zinc–embelin cell is not as high as that of the manganese dioxide based cells, the former gives almost a flat discharge.

The zinc–embelin cell is capable of performing as a secondary battery because the end-of-discharge product of embelin, can be converted back to the original chemical state by charging (Schemes I and II). A discharge coupled with a charging is shown in Figure 4. The cell can be charged at a relatively good efficiency and we have so far obtained 44 cycles with the present system.

The effect of temperature variation on discharge performance is shown in Figure 5. As temperature decreases there is a decrease in the capacity of the battery together with a slight decrease in the cell voltage. At 273 K the total output of the cell is only 60% of the output at room temperature.

3.1. Zeolite modification of embelin

The use of inorganic modifiers in electrode modification has gained importance in the recent past. Early example of these inorganic modifiers include metal oxide parti-
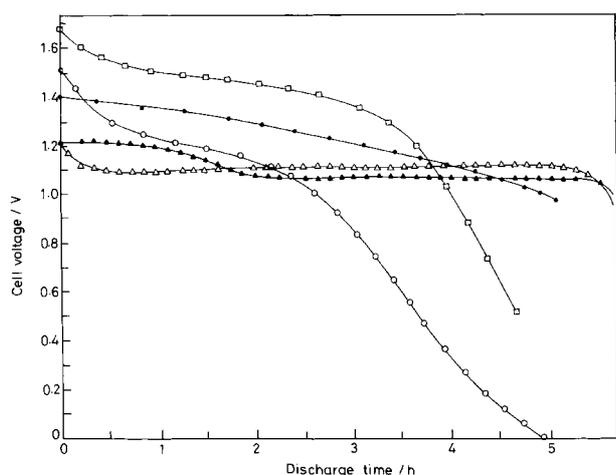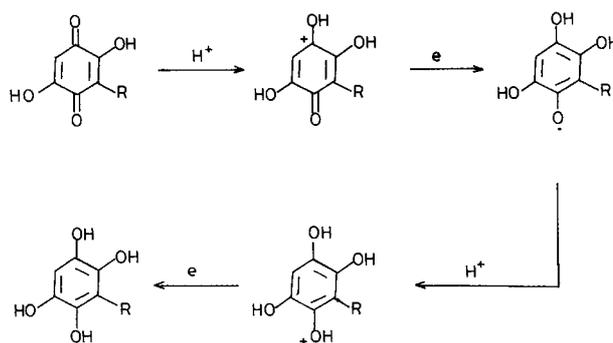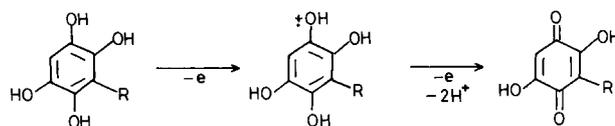
Scheme I. Reduction of embelin during discharge.

cles [8], clays [9, 10] zeolites [11, 12] porous aluminium oxide films [13] and metallo–cyano derived lattice [14–17]. Zeolites are attractive materials for electrode modification because they are ion-exchange materials, they have molecular sieving properties and they are potential catalysts. Several examples of the application of zeolites and its analogues in electrochemical phenomena can be quoted [18–30]. Recently we reported [6] the zeolite modification of a chloranil cathode in a zinc–chloranil secondary battery. The discharge curves of the battery, with and without zeolite modification, are shown in Figures 6 and 7, respectively. Zeolite modification brings about a remarkable improvement in the cycle life of the zinc–embelin cell reaching 84 cycles in contrast to 44 cycles in the absence of zeolite. In the present study, the zeolite used was a calcined rare earth Y zeolite obtained by the cation exchange of commercial Y zeolite using mixed rare earth cations. There is no specific reason for using the rare earth zeolite excepting the fact that it was readily available.

The variation of cell voltage with current density is shown in Figure 8. The slope of such a plot can be taken as a measure of the gross internal resistance of the cell. A comparison of the internal resistance value for a cell with zeolite and without zeolite (Table 1) shows that introduction of zeolite increases the internal resistance of the cell.

The infrared spectrum of the organic compound isolated from the end-of-discharge product is shown in Figure 9, curve (b). The spectral pattern is completely different from that of embelin (Figure 9, curve (a)). It can be seen that the absorption characteristic of the

Fig. 3. A comparison of zinc–embelin cell with manganese dioxide based cells. Key: (□ Mg/Mg (ClO$_4$)$_2$/MnO$_2$; (●) Zn/KOH/MnO$_2$; (○) Zn/NH$_4$Cl/MnO$_2$; (▲) Zn/embelin/ZnCl$_2$ + NH$_4$Cl; (△) Zn/ embelin/1.5 M H$_2$SO$_4$.

Scheme II. Oxidation of the discharge product during charging.

800

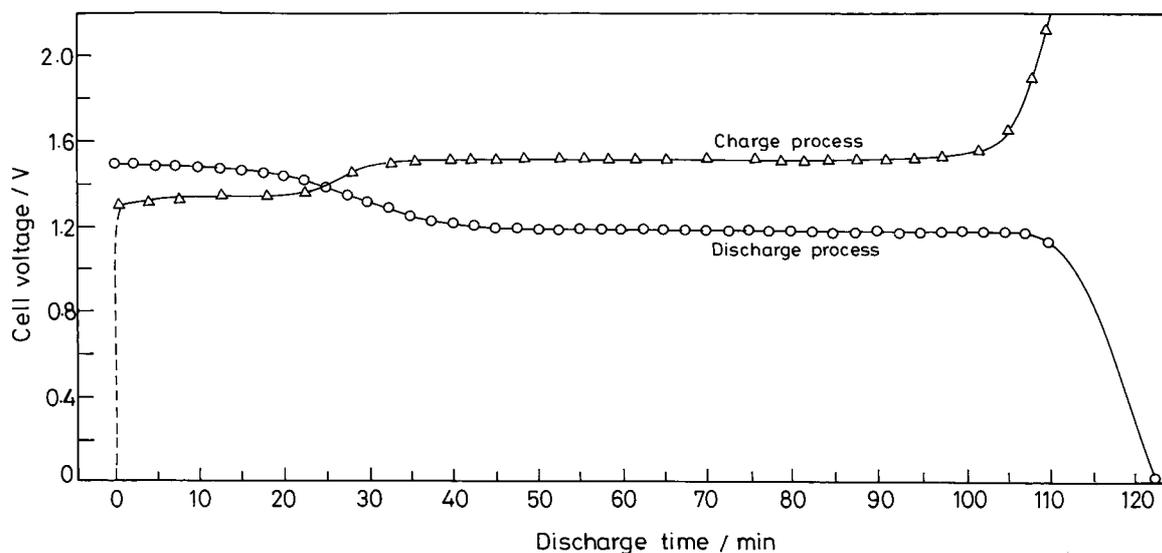*Fig. 4.* A discharge coupled with a charging of a zinc–embelin-ZnCl₂/NH₄Cl cell.

carbonyl (quinone) functions are absent in the spectrum of the product. On the otherhand, frequencies characteristic of OH functionalities, namely at $3400\,cm^{-1}$ and $1110\,cm^{-1}$ are prominent. It is evident, therefore, that the end-of-discharge product corresponds to the reduction product of embelin. The infrared spectrum of the cathode material after charging corresponded to the quinone starting material.

The cyclic voltammograms of the cathode active material (only the organic component) removed from a battery at different stages during discharge are shown in Figure 10. The reversible couple corresponds to the reduction of quinone [31]. As the discharge progressed we observed a reduction in the peak current of the cyclic voltammogram. This observation indicates a reduction in the quantity of the starting material, namely embelin. Although the i_p values of the cyclic voltammograms are roughly equal, they represent only a proportionate increase with the extent of charge because of the different order of dilution as discussed in Section 2.
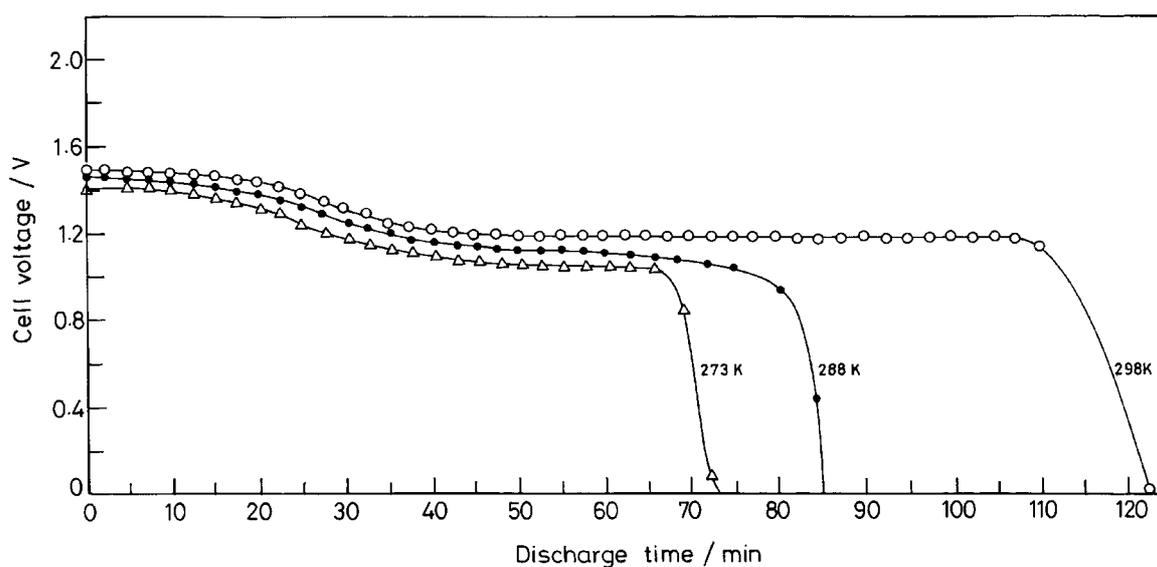

Fig. 5. Effect of temperature variation on the discharge performance of zinc–embelin cell ZnCl₂–NH₄Cl electrolyte (pH 4.7). Current drain 50 mA; compaction pressure 15 t.
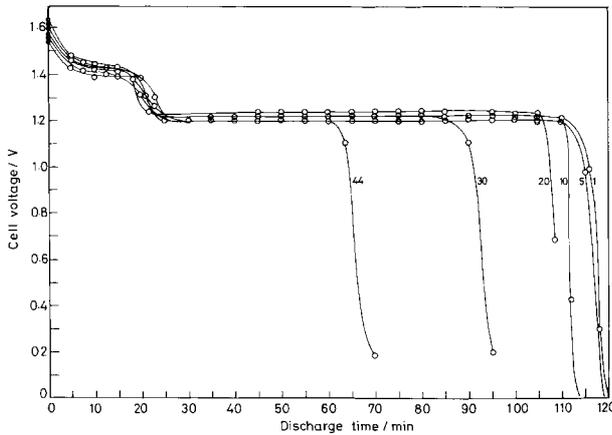
Fig. 6. Discharge curves of zinc–embelin secondary battery at different cycles. Electrolyte: $ZnCl_2/NH_4Cl$, pH 4.7. Numbers represent the number of cycles. Current drain 50 mA.

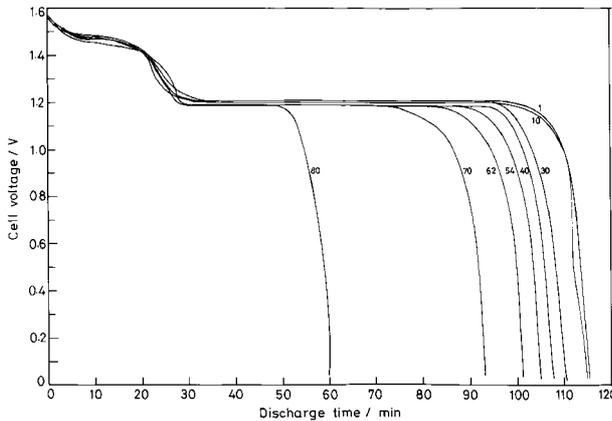*Fig. 7.* Discharge curves of zeolite modified embelin–zinc secondary battery. Electrolyte: $ZnCl_2/NH_4Cl$, pH 4.7. Number represent the number of cycles. Current drain 50 mA; compaction pressure 12 t.

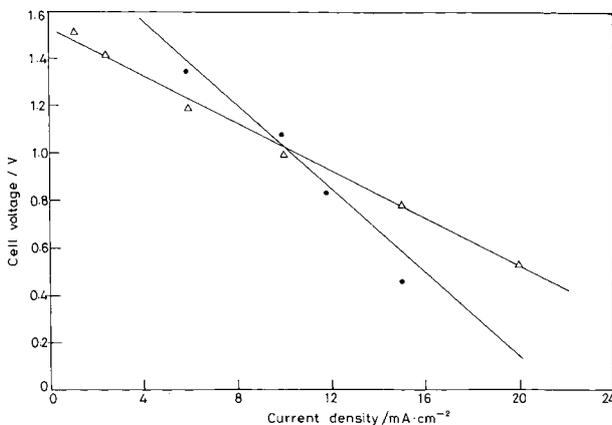*Fig. 8.* Dependence of cell voltage on current drain of a zeolite modified zinc–embelin battery ($\triangle$) 5th cycle, ($\bullet$) 50th cycle. Slopes: ($\triangle$–$\triangle$) 59.3 and ($\bullet$–$\bullet$) 84.7 Ω cm^2.

Table 1. Ampère-hour capacity and gross internal resistance of the zinc–embelin battery at different cycles

Cycles	Capacity/mA h		Gross internal resistance /mΩ	
	without zeolite	with zeolite	without zeolite	with zeolite
1	118	123	50.2	63.5
10	116	116	60.4	67.3
30	98	98	85.7	71.2
40	87	98	91.2	72.4
60	–	98	–	90.0
80	–	70	–	96.0
110	–	–	–	–

The cyclic voltammograms of the cathode material (together with zeolite and colloidal graphite) at different stages during the charging process (Figure 11) show an increase in the peak current values, with the progress of charge, indicating the regeneration of the starting material during charging. As can be seen from the cyclic voltammogram, $i_pa = i_pc$; this feature is characteristic of a reversible reaction and quinones are classic examples for reversible redox chemistry [31].

Shepherd's model of curve fitting [32] was employed to calculate the internal resistance as well as the available active material of the zinc–chloranil battery at different cycles. The values are listed the Table 2.

The effects of compaction pressure on discharge performance of embelin in the presence of zeolite are shown in Figure 12. Both high and low pressure do not seem to be useful as they bring about a decrease both in
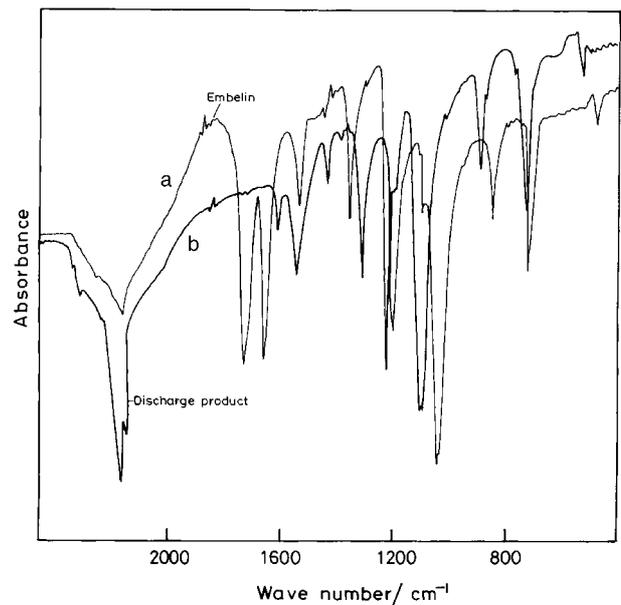

Fig. 9. Infrared spectra of (a) embelin and (b) end-of-discharge product.
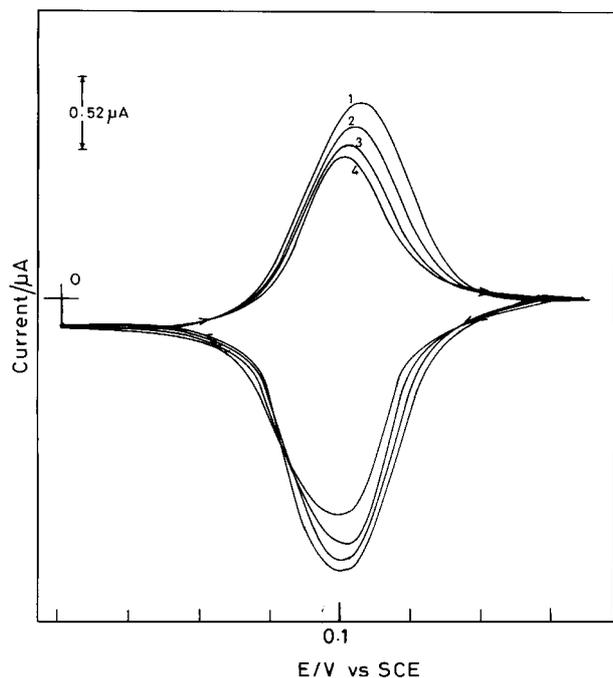
Fig. 10. Cyclic voltammogram of the cathode material extracted from the cathode mix at various stages during discharge; time of arresting the discharge for collection of the cathode material. (a) 30 min, (b) 50 min, (c) 80 min and (d) 105 min. Medium: 50% dioxan, B.R. buffer, pH 4.7; sweep rate 50 mV s^{-1}. Cathode mix has been extracted with 25 ml of DMF it was diluted further and described in Section 2.
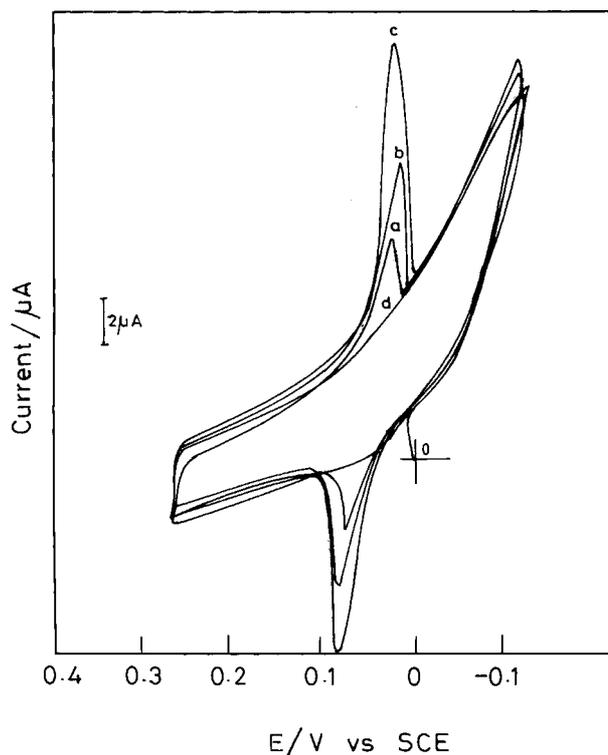

Fig. 11. Cyclic voltammogram of cathode mix at different stages during the charging process. (a) 5 min, (b) 8 min and (c) 12 min. (d) is the base line of zeolite + colloidal graphite blend. Medium: 50% dioxan, B.R. buffer, pH 4.7; sweep rate 50 mV s^{-1}.

the capacity and voltage of the cell. An optimum pressure of 12 t seems to be adequate for good performance.

4. Conclusion

We have observed that embelin, a plant substance, extracted from the plant *Embelier libes* (from the Kerala State of India) shows battery activity. Rechargeable cells of embelin using zinc positive were constructed and investigated under conditions of different parametric variations. We have so far obtained 44 cycles with such a cell.

Zeolite modification of embelin improves the efficiency of embelin as a negative cathode in a zinc–embelin secondary battery. We observed an improved cycle life performance of the battery, reaching 84 cycles in contrast to 44 cycles in the absence of zeolite modification; obviously, zeolite confers efficiency by effecting a more complete reduction of embelin during discharge and a more complete oxidation of the reduced embelin to embelin during charging. The mechanism of participation of zeolites in organic reactions is now well understood. The participation is through (a) stabilization of short lived free radicals, (b) Bronsted acidity and (c) product selectivity and the mode of assistance being dependent on the Si/Al ratio. Therefore, a study of the

Table 2. Characteristics of zinc–embelin cell as derived from Shepherd's curve fitting

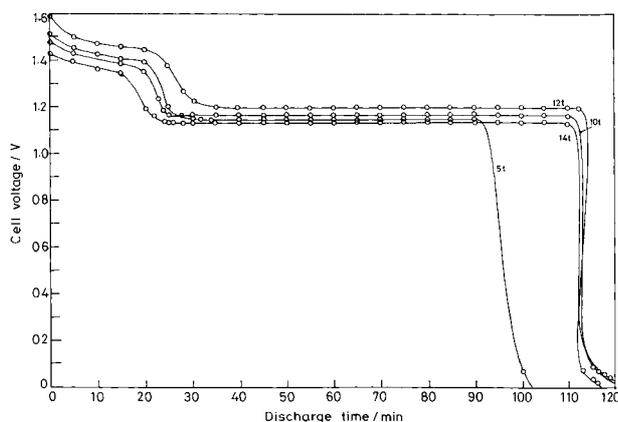|	10th Cycle		40th Cycle	
	without zeolite	with zeolite	without zeolite	with zeolite
Closed circuit potential/V	1.20	1.22	1.20	1.22
Mean available active material/mA min cm^{-2}	0.033	0.041	0.020	0.031
Coefficient of polarization/Ω	0.05	0.057	0.06	0.067
Internal resistance of the cell/Ω	0.464	0.597	1.111	0.900

Fig. 12. Effect of compaction pressure on the performance of zinc–zeolite modified embelin secondary battery. Electrolyte: $ZnCl_2/NH_4Cl$, pH 4.7. Numbers represent pressure in tonnes; constant current drain 50 mA.

performance of the zeolite modified embelin negative under conditions of different Si/Al ratio is necessary in order to fabricate batteries of practical importance.

There is an increase in the internal resistance of the cell upon zeolite modification (up to 15 cycles). However, the increase is not found to be detrimental to the capacity of the battery, upto 84 cycles; probably the large pore size zeolite enables a more uniform distribution of colloidal graphite, facile access of the electrolyte and prevents gas locking in the cathode. Unfortunately the cathode loses capacity on cycling beyond 84 cycles. The cause may lie in the degradation of the cathode material. We have also identified both quinone and the phenol in appreciable quantities in the electrolyte.

It is possible that there was some shedding of the cathode material and/or their leaching into the electrolyte. It is also possible that the zeolite matrix is subjected to a slow degradation, in the acidic (pH 4.7) electrolyte medium. A future zeolite candidate may be formed from a different Si/Al ratio to be able to withstand lower pH of the solutions of battery environment. Similarly, a separator material of higher mechanical strength, porosity and conductivity could be used in place of cellophane.

Mechanical work imposed (e.g., by grinding or applying pressure) when preparing the zeolite modified electrode is certain to influence the performance of the electrode [15, 33] and the subject deserves further study.

Acknowledgement

References

1. G.A. Rechnitz. *Science*, **214** (1981) 287.
2. M.A. Arnold and G.A. Rechnitz, A.F.P. Turner, I. Karube and G. Witson (Eds), 'Biosensors, Fundamentals and Application' (Oxford University Press, 1980), p. 30.
3. Y. Sato, K. Chikyu and K. Kobayakawa, *Chem. Lett.* (1989) 1305.
4. Y. Sato, A Kotake and K. Kobayakawa, *Denki Kagaku* **62** (1995) 1084.
5. Alt H. Binder, A Kohling and G. Sandstede, *J. Electrochem. Soc.* **118** (1971) 950.
6. D. Kalaiselvi, and R. Renuka, Submitted to *J. Power Sources*.
7. A.J. Bellamy, *Anal. Chem.* **52** (1980) 607.
8. D.C. Freeman Jr, *US Patent 3186 8 75* (1965); *British Patent, 998 948* (1965).
9. M.M. Thackerray and J. Coetzer, *Soild State Ionics* **6** (1982) 135; *German Patent 2 942 764* (1980).
10. Furukawa Battery Co., Ltd. *Japan Patent 83 122 63* (1983); *Chem. Abstr.* **99** (1983) 25450g.
11. T. Inoue, K. Kobayashi and K. Kobayashi and K. Matsuo, *Japan Patent 87 193 060* (1987); *Chem. Abstr.* **108** (1988) 8802g.
12. A. Moor, *German Patent, 1 302 003* (1969); *Chem. Abstr.* **73** (1970) 126473g.
13. M.Crucena, E. Popovice and A. Vasile, *Rom. Patent RO 78 511* (1982); *Chem. Abstr.* **99** (1983) 125685c.
14. K. Miwa, K. Iwayama and H. Fukui, *Japan Patent, 87 241 265* (1987); *Chem. Abstr.* **108** (1988) 24622d.
15. D.R. Rolison, *Chem. Rev.* **90** (1990) 867.
16. D.R. Rolison, C. A. Bessel, M. D. Baker, C. Seneratne and J. Zhang, *J. Phys. Chem.* **100** (1996) 8610.
17. T. Bein and P. Enzel, *Angew. Chem. Int. Ed., (Engl)* **28** (1989) 1692.
18. T. Bein and P. Enzel, *Synth. Metals,* **29** (1989) E163.
19. T. Bein and P. Enzel, *J. Phys. Chem.* **93** (1989) 6270.
20. A.J. Bard and T.E. Mallou, *in* 'Molecular Design of Electrode Surfaces', edited by R. W. Murray, cited in Ref.15.
21. C. Johansson, L. Risinger, L. Fallth and L. Huy, *Sci. Inst.* **49** (1980) 47.
22. R.P. Townsend, *Pure Appl. Chem.* **58** (1986) 1359.
23. J. Sarradin, J. Louvet, R. Mersina and J. Perchon, *Zeolites* **4** (1984) 157.
24. D.W. Breck, 'Zeolite Molecular Sieves: Structure, Chemistry & Use' (Wiley-Interscience, New York, 1974).
25. W.M. Meier and D.H. Olsen, 'Atlas of Zeolite Structure Types' (Juris Press, Zurich, 1978).
26. J.A. Jacobs, 'Carboniogenic Activity of Zeolites' (Elsevier, Amsterdam, 1977).
27. J.B. Peri, *in* 'Catalysis: Science and Technology', edited by J.R. Anderson and R.M. Boudart (Springer-Verlag, Berlin, 1984), p. 191.
28. W.F. Holderich and H. Van Bekkum, *Studies in Surface Science & Catalysis* **58** (1991) 631.
29. V. Ganesan and R. Ramaraj, *Langmuir* **14** (1998) 2497.
30. R.N. Jones and C. Sandorfy, *in* 'Technique of Organic Chemistry', vol. 9. Weissberger (Ed.) (Interscience, London, 1956), p. 463.
31. J. Heyrovsky and P. Zuman, 'Practical Polarography' (Academic Press, New York and London, 1950).
32. C.M. Shepherd, *J. Electrochem. Soc.* **112** (1965) 657.
33. M.D. Baker and C. Senaratne, *in* 'Frontiers of Electrochemistry, vol. 3; Electrochemistry of Novel Materials', edited by J. Lipkowski and P. N. Ross (VCH, New York, 1994), pp 339–380.